Impact of Hyperpolarization-activated, Cyclic Nucleotide-gated Cation Channel Type 2 for the Xenon-mediated Anesthetic Effect

Evidence from In Vitro *and* In Vivo *Experiments*

Corinna Mattusch, Ph.D., Stephan Kratzer, M.D., Martina Buerge, M.D., Matthias Kreuzer, Ph.D., Tatiana Engel, M.S., Claudia Kopp, D.V.M., Martin Biel, Ph.D., Verena Hammelmann, Ph.D., Shui-Wang Ying, M.D., Peter A. Goldstein, M.D., Eberhard Kochs, M.D., Rainer Haseneder, M.D., Gerhard Rammes, Ph.D.

ABSTRACT

Background: The thalamus is thought to be crucially involved in the anesthetic state. Here, we investigated the effect of the inhaled anesthetic xenon on stimulus-evoked thalamocortical network activity and on excitability of thalamocortical neurons. Because hyperpolarization-activated, cyclic nucleotide-gated cation (HCN) channels are key regulators of neuronal excitability in the thalamus, the effect of xenon on HCN channels was examined.

Methods: The effects of xenon on thalamocortical network activity were investigated in acutely prepared brain slices from adult wild-type and HCN2 knockout mice by means of voltage-sensitive dye imaging. The influence of xenon on single-cell excitability in brain slices was investigated using the whole-cell patch-clamp technique. Effects of xenon on HCN channels were verified in human embryonic kidney cells expressing HCN2 channels.

Results: Xenon concentration-dependently diminished thalamocortical signal propagation. In neurons, xenon reduced HCN channel-mediated I_h current amplitude by 33.4 ± 12.2% (at −133 mV; n = 7; P = 0.041) and caused a left-shift in the voltage of half-maximum activation ($V_{1/2}$) from −98.8 ± 1.6 to −108.0 ± 4.2 mV (n = 8; P = 0.035). Similar effects were seen in human embryonic kidney cells. The impairment of HCN channel function was negligible when intracellular cyclic adenosine monophosphate level was increased. Using HCN2$^{-/-}$ mice, we could demonstrate that xenon did neither attenuate *in vitro* thalamocortical signal propagation nor did it show sedating effects *in vivo*.

Conclusions: Here, we clearly showed that xenon impairs HCN2 channel function, and this impairment is dependent on intracellular cyclic adenosine monophosphate levels. We provide evidence that this effect reduces thalamocortical signal propagation and probably contributes to the hypnotic properties of xenon. **(Anesthesiology 2015; 122:1047-59)**

DETAILED mechanisms of how consciousness arises in the brain and how anesthetics induce loss of consciousness are still unknown. During loss of consciousness, the majority of anesthetic drugs reduce thalamic metabolism and blood flow.[1] It is still debated however, whether the thalamus serves as a "consciousness switch" or if thalamic depression occurs as a consequence of decreased cortical activity.[2]

The primary functions of thalamic nuclei are to mediate multimodal integration of information and to relay peripheral sensory information to the cortex.[3,4] Consequently, the thalamus is intensively connected to cortical structures by thalamocortical feed-forward and even to a higher degree by corticothalamic feedback connections.[4,5] The functional state of thalamic neurons is regulated by both inhibitory and excitatory input; excitatory input is provided by ascending activating systems from the brain stem and descending

What We Already Know about This Topic

- The precise mechanism by which xenon produces anesthesia is not clear. Available data indicate that thalamic metabolism is reduced by xenon and that disruption of thalamocortical connectivity might, in part, play a role in xenon anesthesia.
- Thalamic hyperpolarization-activated, cyclic nucleotide-gated cation channels (HCN) are discussed to be key targets of anesthetic effects on consciousness.

What This Article Tells Us That Is New

- In thalamocortical slices, xenon evoked HCN channel–dependent impairment of neuronal excitability and reduced thalamocortical signal propagation.
- In HCN2 knockout mice, the sedative effect of xenon was not observed.
- The data suggest that depression of thalamocortical signal propagation that is in part mediated by HCN2 channels might contribute to the anesthetic action of xenon.

Corresponding article on page 971. Drs. Mattusch and Kratzer contributed equally to this work.

Submitted for publication June 20, 2014. Accepted for publication January 29, 2015. From the Department of Anesthesiology, Klinikum rechts der Isar, Technische Universität München, Munich, Germany (C.M., S.K., M. Buerge, M.K., T.E., C.K., E.K., R.H., G.R.); Department Pharmazie—Zentrum für Pharmaforschung, Ludwig-Maximilians-Universität München, Munich, Germany (M. Biel, V.H.); and Department of Anesthesiology, Weill Cornell Medical College, New York, New York (S.-W.Y., P.A.G.).

 Anesthesiology 2015; 122:1047-59

corticothalamic pathways.[6] Electrophysiologically, the thalamocortical network is characterized by rhythmic burst activity during natural sleep and tonic single-spike activity during wakefulness.[6,7] In thalamocortical relay neurons, hyperpolarization-activated, cyclic nucleotide-gated (HCN) cation channels (primarily HCN2[8]) are highly expressed and are well-known for their regulation of neuronal activity.[9]

The noble gas xenon is an inhaled anesthetic that displays many properties of an ideal anesthetic.[10] Functional imaging studies have demonstrated a depression of thalamic activity during xenon anesthesia.[11] The disruption of thalamocortical connectivity, and hence of information transfer from the periphery to the cortex, might be an essential neuronal feature of the xenon-induced anesthetic state. Although both intravenous[12] and volatile[13,14] anesthetics reduce excitability of thalamocortical neurons, the neuronal mechanisms underlying the xenon-induced anesthetic state are still under debate.[15–19]

We hypothesized that xenon decreases thalamocortical flow of information as a consequence of reduced intrinsic neuronal excitability resulting from an impairment of HCN channel function. Therefore, we investigated the impact of xenon on thalamocortical signal propagation and thalamic HCN channel function in acutely prepared brain slices from wild-type (WT) and HCN2$^{-/-}$ mice, as well as in human embryonic kidney cells stably transfected with HCN2 channels.

Materials and Methods

Experimental protocols were approved by the Ethical Committee on Animal Care and Use of the Government of Bavaria (Munich, Germany). After anesthetizing male C57Bl/6 mice (P21–P49) with isoflurane, brains were quickly removed and thalamocortical slices (400-μm thickness)[20] including the ventrobasal thalamus were prepared in ice-cold, carbogen-gas (95% O_2/5% CO_2) saturated artificial cerebrospinal fluid (aCSF; pH 7.4) using a vibratome (HM 650 V; Microm International, Germany). Slices used in patch clamp recording experiments were allowed to recover in a storage chamber for at least 1 h at 34°C, where they were continuously perfused with aCSF at a rate of 5 ml/min. The aCSF contained (in mM): NaCl 125, KCl 2.5, $NaHCO_3$ 25, $CaCl_2$ 2, $MgCl_2$ 1, D-glucose 25, NaH_2PO_4 1.25. All experiments were performed at room temperature (20°–25°C).

For optimized preservation of the neuronal network,[21] thalamocortical slices[20] for voltage-sensitive dye imaging (VSDI) experiments were cut in carbogenated sucrose-based aCSF (2.5 mM KCl, 24 mM $NaHCO_3$, 1.25 mM NaH_2PO_4, 234 mM sucrose, 11 mM glucose, 0.5 mM $CaCl_2$, and 10 mM $MgSO_4$). For dye-loading, slices were kept in carbogenated standard aCSF containing the voltage-sensitive indicator dye, Di-4-ANEPPS (7.5 mg/ml; <0.1% DMSO)[22] for 15 min. Afterward, slices were stored for at least 30 min in standard aCSF. In the recording chamber, slices were continuously superfused with carbogenated standard aCSF (2–3 ml/min flow rate). Electrical stimulation (50–100 V; 0.5 ms) was applied to the ventrobasal thalamus using a bipolar concentric electrode, and circular regions of interest (ROI) were manually selected in the cortex. Different concentrations of xenon were investigated in different brain slices for each experiment.

As a measure of neuronal activity, we calculated the fractional change in fluorescence (ΔF/F) for the ROI (3 × 3 pixels). VSDI was performed on an Olympus BX51WI fluorescence microscope (Olympus, Germany) equipped with a MiCAM02-HR camera (BrainVision, Japan), a XLFluor4X/340 objective (NA 0.28; Olympus) with a 480–550 nm bandpass excitation filter, 590 dichroic and a 590 nm LP emission filter. Acquisition settings were 88 × 60 pixels frame size, 36.4 × 40.0 μm pixel size, and 2.2 ms sampling time. To improve signal/noise ratio, eight acquisitions subsequently recorded at intervals of 15 s were averaged. For all measurements, ΔF/F values were spatially smoothed using a 3 × 3 pixels average filter. In addition, a temporal filter was applied calculating the fluorescence (F) of a pixel at the frame-number (t) using the equitation $F(t) = (F(t - 1) + F(t) + F(t + 1))/3$. Pixelation of images was reduced by the interpolation function of the MiCAM02 software (BrainVision).

Infrared videomicroscopy[23] (Zeiss, Germany) was used to visualize thalamocortical neurons in the ventrobasal complex, which were identified electrophysiologically according to their depolarizing sag and after-depolarization potential in response to a hyperpolarizing current step.[12] In addition to the electrophysiological characterization, the morphology of some of the recorded neurons was verified using neurobiotin-cy3-streptavidin staining.[24] For all single-cell recordings in acute slices, whole-cell recordings were performed with pipettes with an open tip resistance of 4–6 MΩ when filled with an intracellular solution containing (in mM): K-D-gluconate 95, K_3-citrate 20, BAPTA 3, HEPES 10, $MgCl_2$ 2, $NaCl_2$ 10, $MgCl_2$ 1, $CaCl_2$ 0.5, Mg_2-ATP 3, and Na_2-GTP 0.3.

To characterize the morphology of recorded neurons 0.5% neurobiotin (Vector Laboratories, USA) was included in the patch pipette. Neurobiotin was iontophoretically injected into the soma using hyperpolarizing current pulses (–90 to 130 pA; 500 ms). For visualization of neurobiotin-filled cells, the slices were fixed for at least 24 h in 4% paraformaldehyde at 4°C and incubated for 1–2 days in 1:200 streptavidin-conjugated indocarbocyanin (cy3; Jackson Immunoresearch Laboratories, USA) in 0.1 M phosphate-buffered saline pH 7.4 with 2% Triton-X-100. Images were acquired using a confocal microscope (Zeiss) equipped with a krypton-argon laser. Excitation was at 568 nm, and emission filters were set to 590–610 nm for cy3.

Whole-cell patch clamp recordings were obtained using a switched voltage-clamp amplifier (SEC 10L; NPI Electronic, Germany) with switching frequencies of 60–80 kHz (25% duty cycle). Series resistance was continuously monitored. In the voltage-clamp mode, I_h currents were activated by hyperpolarizing steps from a holding potential of –43

to –133 mV in 10-mV increments. To account for the fast activation kinetics of I_h and to increase the stability of the whole-cell recordings, the pulse length was shortened by 500 ms with increasing hyperpolarization (1.5-s pulse length at –133 mV). Tail current amplitude (I_{tail}) was normalized to the tail current observed at the most hyperpolarized membrane potential (–133 mV) to estimate steady-state activation p(V). Voltage dependency of steady-state activation ($V_{1/2}$) is well described by a Boltzmann distribution and time constants (τ) were determined by fitting currents evoked during hyperpolarizing steps to a biexponential function. To determine p(V), the equation $p(V) = (I - I_{min})/(I_{max} - I_{min})$ was used with I_{max} being the tail current amplitude for the voltage step from –133 to –103 mV and I_{min} for the voltage step from – 43 to – 103 mV.

Liquid junction potentials were calculated based on intracellular and bath solutions and off-line correction was performed. To inhibit inwardly rectifying potassium channels and to block two-pore-domain acid-sensitive K^+ (TASK) channels, some recordings were performed in the presence of 150-μM Ba^{2+}. The HCN-channel antagonist ZD7288 [4-(N-ethyl-N-phenylamino)-1, 2-dimethyl-6-(methylamino) pyridinium chloride] was directly applied in the external recording solution.

Single-cell recordings of I_h currents in human embryonic kidney (HEK) 293 cells stably transfected with murine HCN2 (mHCN2) channels[25] were performed using the same voltage protocol as in the slice recording experiments except that the extracellular solution contained (in mM) NaCl 125, KCl 2.5, HEPES 30, $CaCl_2$ 2, $MgSO_4$ 2, D-glucose 25, NaH_2PO_4 1.25.

Current-clamp recordings were performed from thalamocortical neurons. Intracellular current pulse injection (–500 pA; 500 ms) evoked the depolarizing sag in the membrane potential in thalamocortical neurons, and the sag amplitude was determined as the difference between the peak hyperpolarization and the steady-state value. The rebound burst delay was measured as the time from the start of repolarization (the end of a hyperpolarizing current pulse) to the peak of the first action potential (AP).

All current responses were amplified, low-pass filtered (3 kHz), digitized (ITC-16 Computer Interface, Instrutech Corp., USA) with a sampling frequency of 9 kHz, and stored on a hard drive (Power Macintosh G3 computer, data acquisition software Pulse version 8.5; HEKA Electronic GmbH, Germany).

The effect of xenon on the basal level of cyclic adenosine monophosphate (cAMP) was investigated in mHCN2-HEK cells with a standard protocol for cell lysate described in a commercially available enzyme-linked immunosorbent assay kit (complete cAMP ELISA kit; Enzo Life Sciences, Germany). Before the experiment, cell samples were matched according to the cell concentration, assessed by cell counting with a Neubauer chamber. Therefore, after pairwise matching, cell samples were regarded as dependent samples. Cell-culture medium was replaced with aCSF, which was continuously saturated with either carbogen (control-group) or carbogen and 65% xenon (xenon-group) for 15 min. Subsequently, cells were rapidly lysed in hydrochloric acid (0.1 M), and the cAMP level was determined with the ELISA kit according to the ELISA kit protocol.

For all VSDI and patch-clamp experiments, the aCSF was saturated with carbogen-gas. Xenon was applied to the aCSF by aeration of the reservoir with a mixture of xenon (in different concentrations) and nitrogen additionally to the saturation of the aCSF with carbogen. Gases were applied at a flow rate of 0.3 to 0.5 l/min to the aCSF reservoir. Concentration of dissolved xenon obtained from saturation of the aCSF with 18% (0.6 mM), 30% (1.1 mM), and 65% xenon (1.9 mM) was measured by headspace gas chromatography (Harlan Laboratories Ltd., Switzerland). Concentration of dissolved xenon after saturation with 100% xenon (2.8 mM) was extrapolated from the measured values.

The sedative property of xenon was tested by measuring spontaneous locomotor activity.[26] Mice were acclimated to the experimental room overnight. On the experimental day, the animal to be tested was placed in a box (40 × 20 × 20 cm), which was connected to a gas cylinder (xenon: O_2; 70:30%). The experimental box was divided into a grid pattern, and using a VideoMot2 system (TSE, Germany), the number of lines crossed was measured for the initial phase (first 5 min after being placed in the box). After this initial phase of adaptation, xenon/O_2 gas was injected into the chamber at a flow rate of 0.5 l/min, and spontaneous activity recorded for an additional 5 min following which the mouse was returned to its home cage. For every animal, the ratio of lines crossed/total lines crossed was compared. The xenon-mediated effect was calculated as the ratio of lines crossed after xenon treatment to the lines crossed under basal conditions.

All gas mixtures were purchased from Linde AG (Unterschleissheim, Germany). All salts and chemicals were purchased from Sigma-Aldrich (Germany), except for CGP35348 (Novartis Laboratories, Switzerland) and ZD7288 (Tocris Cookson Inc., Germany).

Statistical Analysis

For all statistical evaluations, IBM SPSS Statistics version 22 (IBM Deutschland GmbH, Germany) was used. The rationale for why each sample size was used was based on previous experience.

For evaluation of VSDI recordings, the average of eight recordings was analyzed. The curve fit for the fast depolarization-mediated signals (FDS) concentration–response relationship was calculated using the Hill equation. All slices that showed specific cortical depolarization upon electrical thalamic stimulation were included in the analysis. For analysis of the patch-clamp and ELISA experiments, data were tested for normal distribution using Kolmogorov–Smirnov test. Statistical significance was then determined using paired *t* tests for normally distributed samples, and the Wilcoxon signed-rank test for samples that were not normally

distributed. For patch-clamp experiments, all cells were included in the analysis if they did not meet one of following exclusion criteria: (1) no GΩ seal resistance, (2) initial resting membrane potential below −50 mV; (3) unstable series resistance or holding current (>20% change); (4) no stable baseline conditions.

All statistical tests were performed on a two-sided level of significance of 5%. Numerical data are presented as the mean ± SEM with the number of experiments (slices) indicated, if not stated otherwise. If error bars are not visible in graphs, the bars are smaller than the symbol size. Given the nature of the performed experiments, the experimenter was not blinded to the experimental conditions.

Results

In the first set of experiments, we determined the effect of xenon on thalamocortical signal propagation using VSDI recordings). Stimulation was applied to the ventrobasal thalamus and cortical ROIs randomly selected (fig. 1A). Xenon reduced cortical depolarization upon thalamic stimulation (fig. 1B). The effect of 1.9 mM xenon on thalamocortical signal propagation showed only poor recovery upon washout of xenon (fig. 1C). Application of xenon at different concentrations revealed that the effect of xenon on thalamocortical network activity is concentration dependent (extrapolated half-maximum IC_{50}: 2.89 mM; fig. 1D). In accordance with previous results,[27] the neuronal activity observed in VSDI recordings is mainly fed by glutamatergic projections and could be completely blocked by tetrodotoxin application (data not shown).

A decreased thalamocortical flow of information in the presence of xenon could be a consequence of reduced intrinsic neuronal excitability. Therefore, we first determined the effect of xenon on neuronal membrane biophysics. Thalmocortical neurons in the ventrobasal complex were characterized according to their depolarizing sag and after-depolarization in response to hyperpolarizing current injection (fig. 2A). In addition, the morphology of some of the recorded neurons was verified using neurobiotin-cy3-streptavidin staining (fig. 2B). The current–voltage relationship determined by current injection into the recorded cells

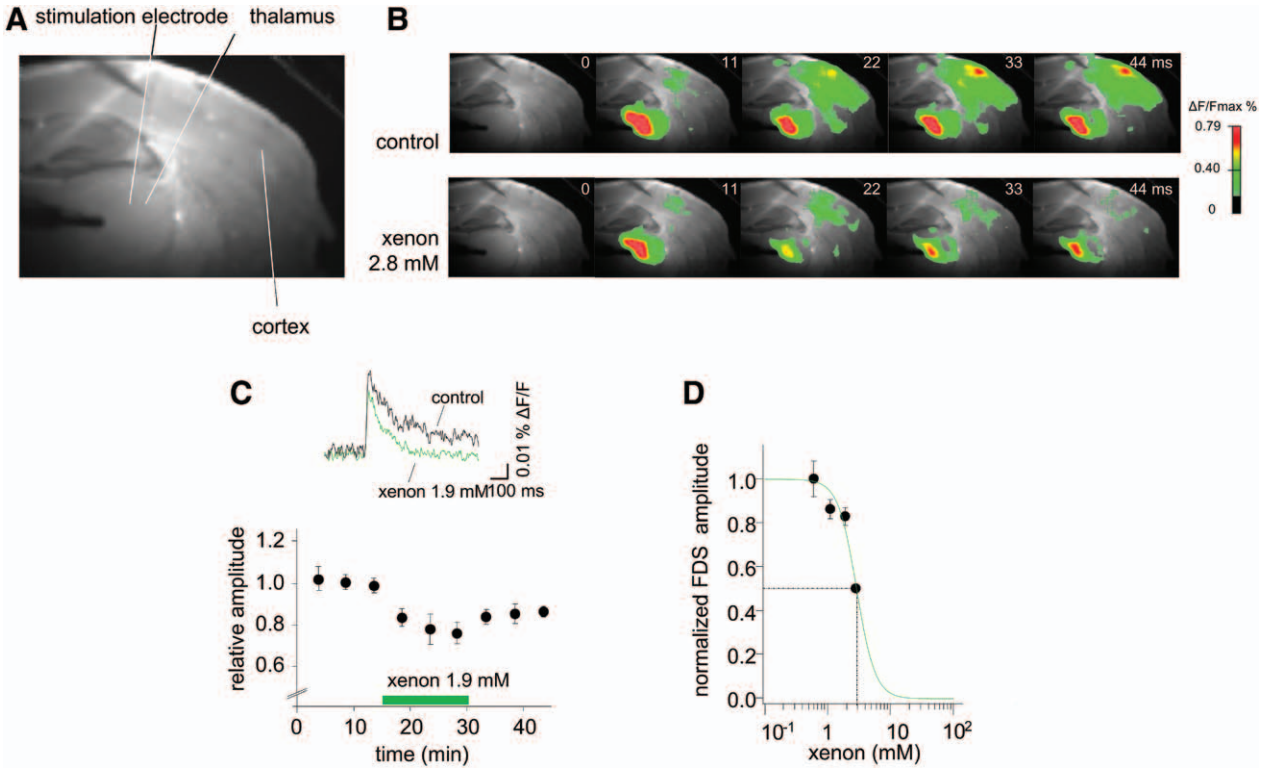

Fig. 1. Xenon dose-dependently reduces thalamocortical signal propagation. (*A*) Topographical overview of thalamocortical slices. The cortical stimulation electrode was used to specifically test integrity of the cortical network at the beginning and the end of every experiment. (*B*) Representative filmstrip of an experiment with thalamic stimulation in the absence (control) and presence of xenon (2.8 mM). (*C*) Representative fast depolarization-mediated signal (FDS) traces in the absence and presence of xenon (1.9 mM) (*top*). Averaged data (*bottom*) indicate that xenon decreased FDS amplitude induced by thalamic stimulation to 83.1 ± 4.1% of control with partial reversibility (n = 7; $P < 0.001$). (*D*) The xenon-mediated effect on thalamocortical signal propagation was concentration dependent. Xenon decreased FDS peak amplitude (relative to control): 0.6 mM: 100.2 ± 8.1%; n = 3; $P = 0.936$; 1.1 mM: 86.4 ± 4.4%; n = 4, $P = 0.022$; 1.9 mM: 83.1 ± 4.1%; n = 7; $P < 0.001$; and 2.8 mM: 50.2 ± 1.5%, n = 4; $P < 0.001$. FDS peak amplitudes were reduced by xenon with an extrapolated half-maximum IC_{50} 2.89 mM (indicated by *dotted lines*; Hill coefficient, −3.5). Each data point represents the mean ± SEM.

was modulated by xenon. In the presence of 1.9 mM xenon current injections of −90 to −50 pA led to further hyperpolarization (when applied at membrane potentials more negative than −50 mV) because of the inhibition of HCN channels and the loss of the inward current required to shift the membrane potential toward more depolarized levels (fig. 2C). Xenon had no effect on resting membrane potential (−62.5 ± 2.2 mV *vs.* −63.2 ± 2.2 mV; n = 12; P = 0.401; fig. 2D). AP firing was observed when cells were depolarized to −44.0 ± 3.1 mV under control conditions; xenon did not affect this threshold (−40.7 ± 4.7 mV; n = 6; P = 0.137; fig. 2E). Under control conditions, a current injection of +90 pA produced tonic AP firing with a mean frequency of 40.2 ± 4.2 Hz; xenon application did not change AP frequency (40.4 ± 3.6 Hz; n = 14; P = 0,153; fig. 2F). Input resistance (R_{in}) was 243.9 ± 23.6 MΩ under control conditions and 392.3 ± 46.6 MΩ in the presence of 1.9 mM xenon (n = 18; P < 0.001; fig. 2G).

The HCN channel-mediated current, I_h, helps to set membrane potential and contributes to the generation of oscillatory activity.[12] Therefore, the observed reduction of thalamocortical signal propagation and R_m-increase might result from xenon-mediated inhibition of HCN channel function. The application of xenon (1.9 mM; ≈0.8 minimum alveolar concentration [MAC]) led to a significant shift in the voltage dependence of I_h activation to more hyperpolarized membrane potentials (fig. 3). Under control conditions, half-maximum voltage activation ($V_{1/2}$) for I_h was −98.8 ± 1.6 mV, whereas in the presence of xenon $V_{1/2}$ was −108.0 ± 4.2 mV (n = 8; P = 0.035; fig. 3E). In addition, in the presence of xenon, maximum current amplitude (at −133 mV) was decreased by 33.4 ± 12.2% relative to control (n = 7; P = 0.041; fig. 3F). The application of the selective HCN channel antagonist 4-(N-ethyl-N-phenylamino)-1,2-dimethyl-6-(methylamino) pyridinium chloride (ZD7288; 100 μM), which induces sedation when it is parenterally administered in high doses to rodents,[28] decreased maximum I_h current amplitude by 87.1 ± 2.1% (at −133 mV; n = 8; P < 0.001; data not shown).

The HCN2 isoform is the predominant HCN channel expressed in thalamocortical neurons,[8] and HCN2 gating is cAMP-sensitive such that binding of cAMP

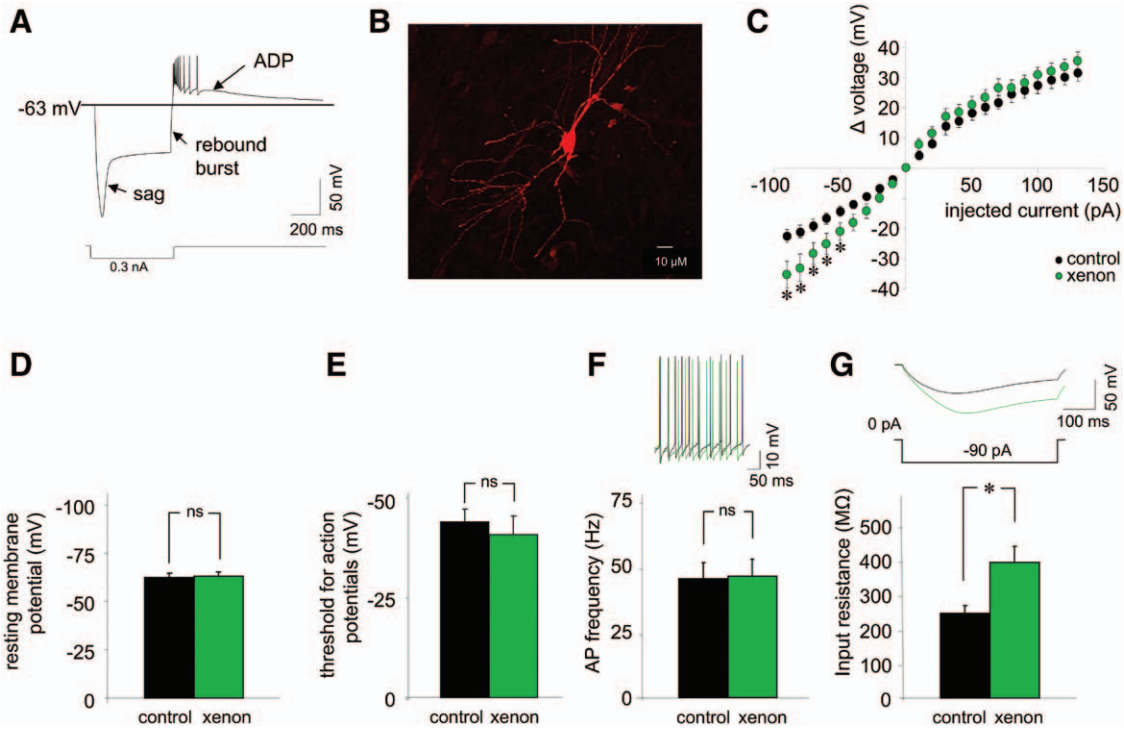

Fig. 2. Characterization of thalamocortical neurons and the effect of xenon on electrical membrane properties. (*A*) Membrane voltage responses resulting from hyperpolarizing direct current injection (protocol shown below) of thalamocortical neurons are characterized by a prominent rectification in the membrane potential ("sag"), low-threshold Ca^{2+} spike rebound burst firing, and after-depolarization potential (ADP). (*B*) Neurobiotin-cy3-streptavidin staining of a thalamocortical neuron. (*C*) Currents from −90 pA to +90 pA (10-pA increments) were injected into thalamocortical neurons and the resulting change (ΔV) in the membrane potential (resting membrane potential was referred to as ΔV = 0 mV) was measured. 1.9 mM xenon significantly increased (*P < 0.05) ΔV over the range of current injection from −90 to −50 pA. (*D*) Recordings from thalamocortical neurons in the current-clamp mode revealed xenon did not affect the resting membrane potential. ns = not significant. (*E*) In the presence of xenon, the threshold for action potential generation remained unchanged. (*F*) Xenon did not alter the frequency of action potential (AP) firing induced by depolarizing current injections. (*G*) Xenon (1.9 mM) significantly (*P < 0.001) increased neuronal input resistance as measured by injection of hyperpolarizing current (current protocol shown below representative voltage traces).

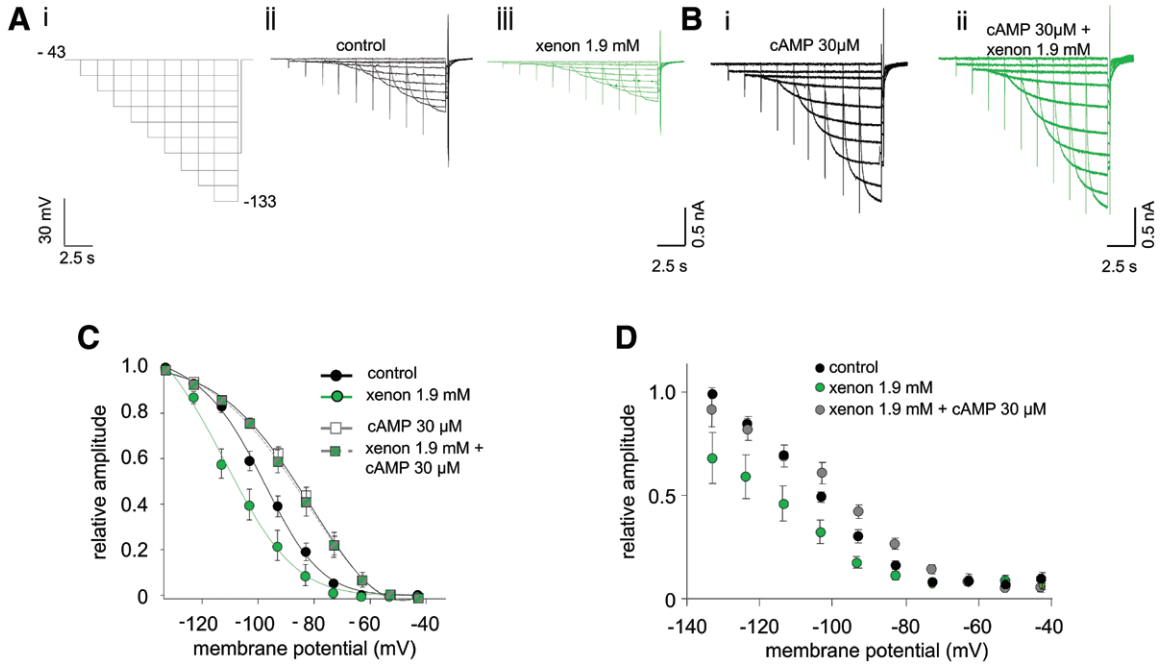

Fig. 3. Xenon-mediated impairment of hyperpolarization-activated, cyclic nucleotide-gated cation (HCN) channels in thalamocortical neurons is cAMP dependent. (*A*, *B*) Representative current trace families ([i] voltage protocol) from a thalamocortical neuron under control conditions (ii), in the presence of 1.9 mM xenon (iii), in the presence of 30 μM cyclic adenosine monophosphate (cAMP; *Bi*) plus 1.9 mM xenon (*Bii*). (*C*) In thalamocortical neurons, the application of xenon (1.9 mM) led to a significant left-shift in the half-maximum activation voltage ($V_{1/2}$). In contrast, inclusion of cAMP (30 μM) in the intracellular solution produced a significant right-shift in the $V_{1/2}$. Xenon application did not reverse the effect of cAMP on the $V_{1/2}$ When cAMP (30 μM) was present in the intracellular pipette solution, $V_{1/2}$ was unchanged during xenon application (–83.1 ± 2.4 mV *vs.* –86.2 ± 1.6 mV; n = 6; P = 0.595). (*D*) Application of 1.9 mM xenon decreased maximum I_h current amplitude by 33.4 ± 12.2% (when the cell was hyperpolarized to –133 mV; n = 7; P = 0.041). The HCN channel antagonist ZD7288 (100 μM) markedly reduced I_h currents by 87.1 ± 2.1% (–133 mV; n = 8; P < 0.001). Xenon did not affect I_h current amplitude in the presence of cAMP.

facilitates channel activation.[29,30] Consequently, we examined whether the effect of xenon is dependent on the level of intracellular cAMP. Experiments were performed under the same conditions as above, except for the addition of a saturating concentration of cAMP (30 μM[31]) to the intracellular solution (fig. 3C). The addition of cAMP (30 μM) significantly shifted the $V_{1/2}$ toward more depolarized values (–86.2 ± 1.6 mV; n = 6; P < 0.001; fig. 3E). Under these conditions, xenon affected neither I_h current amplitude nor the $V_{1/2}$, (n = 5; P > 0.05; fig. 3, E and F). These data suggest that xenon may inhibit HCN channels by either decreasing intracellular cAMP or by competing with cAMP for its binding site.

To examine whether the xenon-induced impairment of HCN channels leads to decreased neuronal excitability, we performed current-clamp recordings from thalamocortical neurons. The characteristic depolarizing sag in the membrane potential observed in thalamocortical neurons in response to membrane hyperpolarization is mediated by an HCN2-dependent I_h conductance.[8] Consistent with previous observations in thalamocortical neurons,[12] sag amplitude was found to correlate with delay time of rebound spike firing (data not shown). We next examined the effect of xenon on sag amplitude and rebound delay. The application of xenon (1.9 mM) decreased the sag amplitude (57.1 ± 12.4%; n = 5; P = 0.026, fig. 4A) and increased the rebound delay (139.5 ± 8.8%; n = 6; P = 0.011; fig. 4B) in a cAMP-dependent manner. The application of ZD7288 (100 μM) in addition to xenon had little further effect on either sag or delay time (data not shown).

In thalamocortical neurons, the HCN channel isoforms HCN2 and HCN4 are highly expressed and I_h currents are primarily mediated by HCN2 channels.[8] The activation time constant τ_{fast} for I_h in thalamocortical neurons hyperpolarized to –133 mV was 178.7 ± 10.8 ms (n = 6). A previous study describes an activation constant for HCN2 in TC-neurons of mice of 460 ms at –100 mV ms.[12] The difference to our time constant may arise from the fact that our time constant was determined at a more hyperpolarized membrane potential because dependence of time constants on the membrane potential has been previously described.[30] To confirm the effect of xenon on the HCN2 isoform, we performed experiments using HEK293 cells in which murine HCN2 (mHCN2) channels were heterologously expressed (fig. 5).

Xenon shifted the $V_{1/2}$ from –94.1 ± 0.8 mV to –98.5 ± 1.5 mV (n = 11; P = 0.017; fig. 5E) and reduced I_h current amplitude by 16.1 ± 3.9% (n = 10; P = 0.006; fig. 5F) for

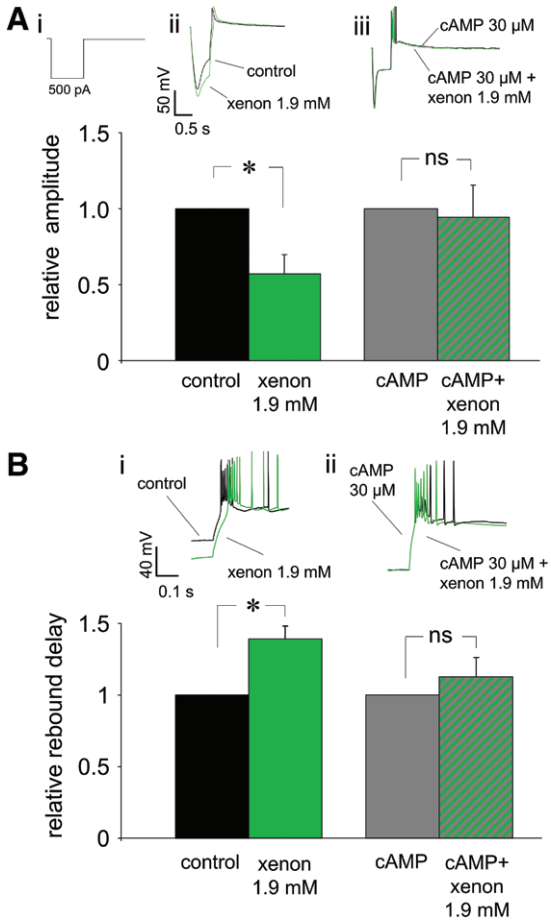

Fig. 4. Effects of xenon on membrane voltage sag and rebound burst delay in thalamocortical neurons. (*A*) Current protocol (i) and exemplar membrane voltage traces (ii) from thalamocortical neurons in the absence and presence of xenon (as indicated) with (iii) and without (ii) the inclusion of cyclic adenosine monophosphate (cAMP) in the pipette solution. Application of xenon reduced sag amplitude to 57.1 ± 12.4% of control (n = 5; $P = 0.026$). With cAMP (30 μM) in the pipette solution, xenon did not impair sag amplitude. (*B*) The application of xenon increased rebound delay to 139.5 ± 8.8% of control (n = 5; $P = 0.011$). With cAMP (30 μM) in the pipette solution, xenon did not change rebound delay (i) exemplar voltage traces from different cells as in *A* with (ii) and without (i) inclusion of cAMP (30 μM) in the pipette solution. *$P < 0.05$; ns = not significant ($P > 0.05$).

currents measured at a membrane potential of –133 mV. Similar to the experiments in thalamocortical neurons, inclusion of cAMP (30 μM) to the pipette solution shifted $V_{1/2}$ to the right (–78.5 ± 1.8 mV; n = 11). Under these conditions, xenon had no effect on either the $V_{1/2}$ or I_h current amplitude for current responses recorded from mHCN2 channels (–76.8 ± 1.7 mV; n = 11; $P = 0.831$; 0.8 ± 4.9% n = 10; $P = 0.864$ at –133 mV; fig. 5, C and D).

The above data suggest that xenon impairs HCN2 channel function in a cAMP-dependent manner; consequently, we investigated the effect of xenon on basal cAMP levels using an ELISA. Baseline cAMP concentrations ranged from 0.5 to 13.6 pmol/ml. After a 15-min application of 1.9 mM xenon, basal cAMP level in mHCN2-HEK cells was 3.9 ± 0.9 pmol/ml (n = 9 samples), which was not statistically significant different from control (5.0 ± 1.4 pmol/ml; fig. 5E).

HCN2 is distributed nearly ubiquitously throughout the most brain regions, with the highest expression in the thalamus.[32] To test the hypothesis that xenon-mediated disruption of thalamocortical signal transfer results from xenon-impairment of HCN2 channel function, we evaluated the effect of xenon on thalamocortical activity propagation in HCN2 deficient mice ($HCN2^{-/-}$) mice[8] (fig. 6A). In WT mice, xenon (1.9 mM) reduced peak amplitudes of cortical FDS evoked by thalamic stimulation to 79.9 ± 6.5% of control (n = 4; $P = 0.046$; fig. 6B). In $HCN2^{-/-}$, the relative amplitude of FDS by thalamic stimulation was unaffected by xenon (93.8 ± 7.5 % of control; n = 5; $P = 0.312$; fig. 6B).

To evaluate xenon-mediated sedation as a function of HCN2 expression *in vivo*, a modified open-field test was performed. Xenon-mediated sedation was rapidly detected within 5 min in WT mice (control [basal]: 0.6 ± 0.0; in the presence of 70% xenon: 0.4 ± 0.0; n = 9; $P = 0.0074$). Because xenon is an HCN2 channel antagonist, and HCN2 channels regulate neuronal physiology in wake-sleep pathways,[33–36] we expected that mice lacking the HCN2 channel would be less sensitive to xenon-mediated sedation than their WT littermates.[37] Indeed, $HCN2^{-/-}$ littermates did not show a difference in the lines crossed under basal conditions compared with xenon treatment (control [basal]: 0.5 ± 0.0; in the presence of 70%: 0.50 ± 0.0, n = 9; $P = 0.2202$, fig. 7A). Evaluating the difference in lines crossed under xenon treatment and comparing it to the lines crossed under basal conditions, the xenon effect is significantly higher in WT mice than in their $HCN2^{-/-}$ littermates (WT, 0.8 ± 0.1; $HCN2^{-/-}$, 1.2 ± 0.1; n = 9; $P = 0.0350$; fig. 7B).

Discussion

In the present study, we demonstrate that xenon disrupts signal propagation in the thalamocortical circuit, resulting from a cAMP-dependent, xenon-mediated impairment in HCN2 channel function. This effect on thalamocortical signal propagation may contribute to xenon's anesthetic properties.

MAC values of xenon in humans range from 63 to 71 vol%.[33,34] The calculated MAC equivalent of dissolved xenon is 2.2 to 2.5 mM using a xenon solubility coefficient of 0.0887.[35] MAC values of xenon for rodents were hyperbaric (1.61 atm[36]). Therefore, the aqueous concentration of xenon (1.9 mM) lies close to the human MAC equivalent, but is below that for rodents. Thus, the effects observed in our murine brain slice preparation may underestimate the effects of xenon in humans.

VSDI signals represent voltage changes originating in neuronal membranes in the dendritic arbor.[37] Because VSDI signals in our thalamocortical slice preparation likely

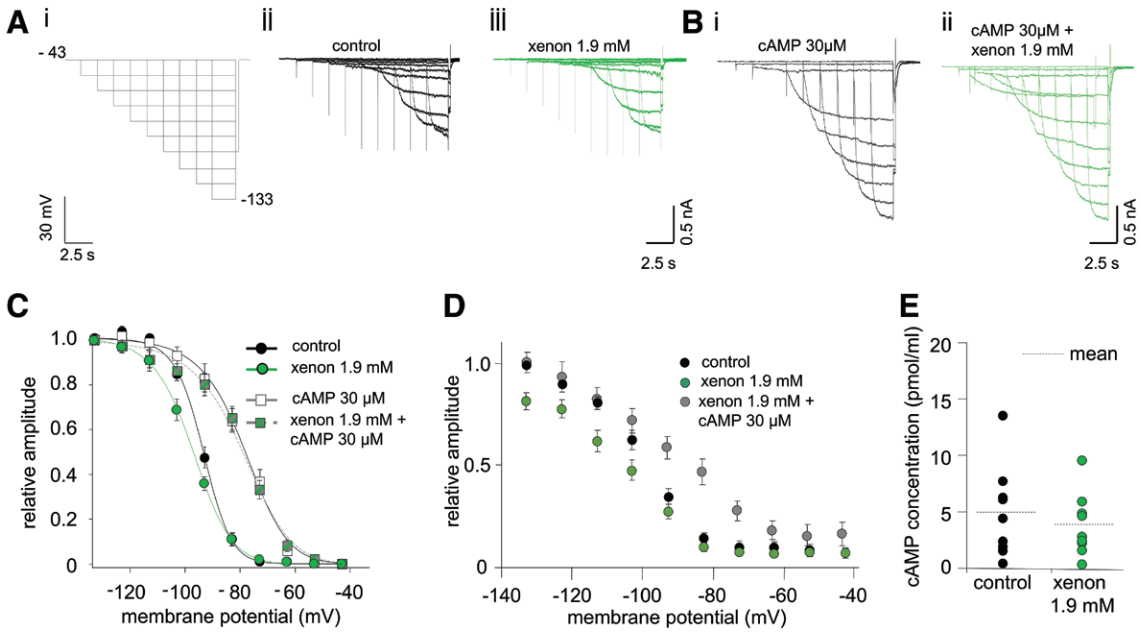

Fig. 5. Xenon-mediated antagonism of murine hyperpolarization-activated, cyclic nucleotide-gated cation channels type 2 (mHCN2) is cyclic adenosine monophosphate (cAMP) dependent. (*A*, *B*) Representative current trace families (*Ai* voltage protocol) from a human embryonic kidney (HEK) 293 cell in which mHCN2 channels were heterologously expressed under control conditions (*Aii*), in the presence of 1.9 mM xenon (*Aiii*), in the presence of 30 µM cAMP (*Bi*) plus 1.9 mM xenon (*Bii*). (*C*) The half-maximum voltage activation ($V_{1/2}$) was shifted from −94.1 ± 0.8 mV under control conditions to −98.5 ± 1.5 mV in the presence of 1.9 mM xenon (n = 11; $P = 0.017$). With 30 µM cAMP in the pipette solution, xenon failed to elicit a shift in the $V_{1/2}$ (cAMP alone: −78.5 ± 1.8 mV *vs.* cAMP + 1.9 mM xenon: 76.8 ± 1.7 mV; n = 11; $P = 0.831$). (*D*) Xenon reduced mHCN2-generated I_h current amplitudes (at membrane potential of −133 mV) by 16.1 ± 3.9% (n = 10; $P = 0.006$). Maximum I_h current amplitudes did not change in the presence of added cAMP (0.8 ± 4.9%; n = 10; $P = 0.86$). (*E*) Basal cAMP levels were determined using enzyme-linked immunosorbent assay in mHCN2-HEK cells. Although there was a small decrease in basal cAMP levels in the presence of xenon, this difference was not statistically significant.

resulted from cortical depolarization in response to thalamic stimulation,[27] our data indicated that xenon concentration dependently reduces thalamocortical signal transmission. In rodents, the ventrobasal complex of the thalamus is considered a first-order relay because it transmits (lemniscal projections[38,39]) directly to the cortex. Because it is of particular importance as a target of anesthetics, we performed single-cell experiments in the ventrobasal complex and placed a stimulation electrode onto the ventrobasal complex for VSDI experiments. Previous studies describe that thalamocortical slice preparation preserves higher order pathways.[40] We cannot exclude that the pulse applied to the ventrobasal complex also stimulated higher-order nuclei of the thalamus, resulting in cortical depolarization. This may limit the reliability of our findings regarding their specificity to the ventrobasal complex. However, expression of HCN2 channels was observed to be weaker in the posterior thalamic nuclear group than in the ventrobasal complex.[41,42] Therefore, our finding of a HCN2 channel-dependent impairment of thalamocortical connectivity is more likely to arise from the ventrobasal regions of the thalamus.

Impaired thalamocortical signal transmission may be a consequence of reduced neuronal excitability of thalamocortical neurons, cortical neurons, or attenuated excitatory neurotransmission. Besides its well-known effects on glutamatergic neurotransmission,[18,19,43] xenon has no impact on intrinsic neuronal excitability in the mouse cortex.[19] However, xenon may still alter neuronal excitability in the thalamus. Thalamocortical neurons generate two patterns of AP firing: (1) synchronized rhythmic oscillatory burst mode and (2) single spike transmission mode.[4,44,45] During wakefulness, thalamocortical neurons are depolarized by afferent input and switch to transition-mode, whereas information is gated through the thalamus to the cortex.[4,46] During sleep, thalamocortical neurons are hyperpolarized and enter the oscillatory burst mode, inhibiting information transfer to the cortex.[47]

Xenon neither affected the resting membrane potential nor the threshold or the frequency of AP firing. When cells were hyperpolarized, xenon reduced neuronal conductance. HCN channels[48] largely mediated neuronal conductance at hyperpolarized membrane potentials. Both HCN channels and two-pore domain K^+ currents influence the excitability of thalamocortical neurons by stabilizing the membrane potential.[49–51] Previous studies showed that volatile anesthetics activate TASK channels,[52,53] resulting in membrane hyperpolarization associated with reduced excitability in thalamocortical neurons.[54,55] Because dual modulation of

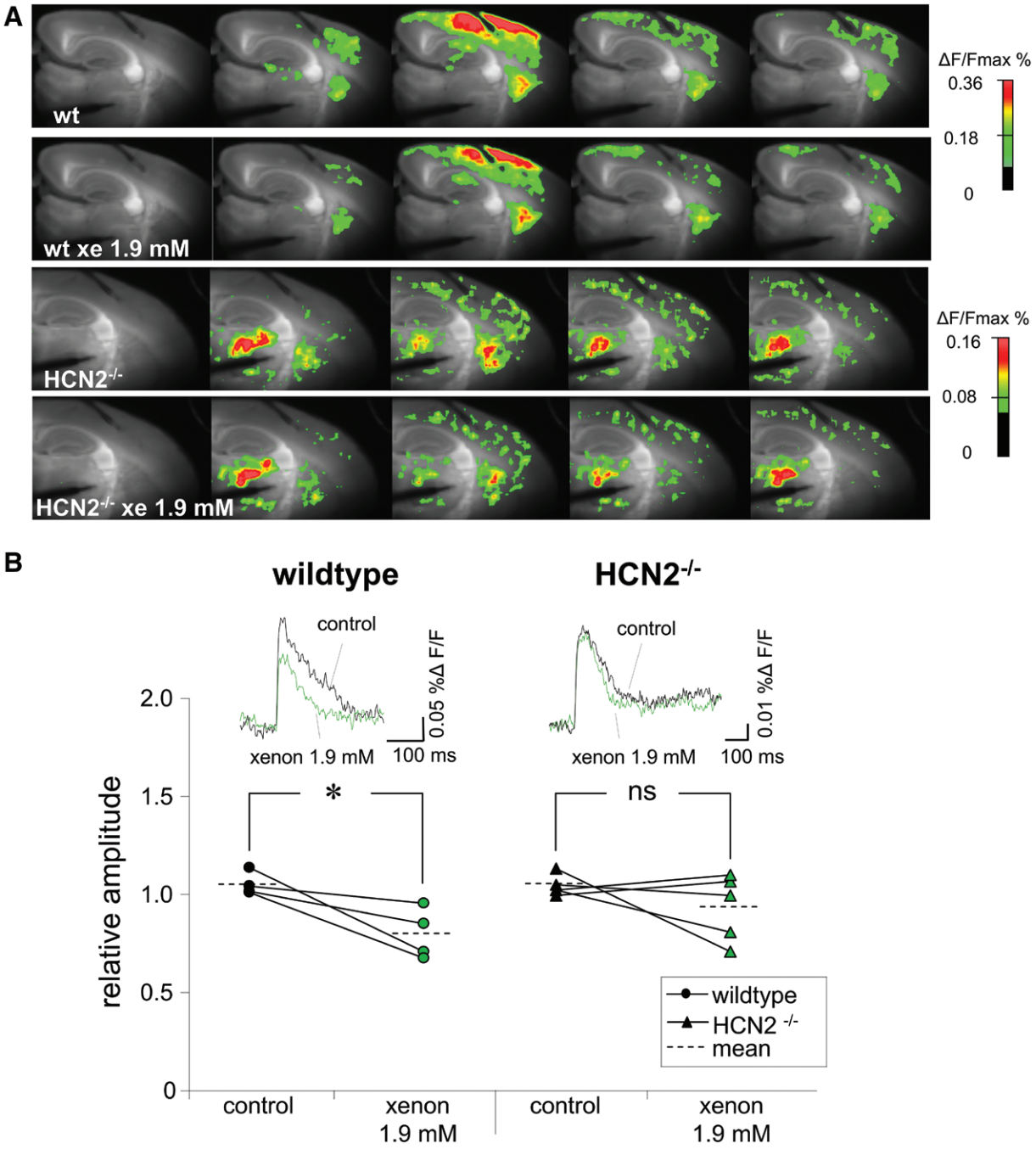

Fig. 6. Expression of hyperpolarization-activated, cyclic nucleotide-gated cation channels type 2 (HCN2) is required for xenon-mediated disruption of thalamocortical signal propagation. (*A*) Representative filmstrips of thalamocortical signal propagation evoked by thalamic stimulation in the presence of xenon (xe) (1.9 mM) in brain slices from wild-type (WT) and HCN2$^{-/-}$ mice. (*B*) In WT mice, xenon (1.9 mM) attenuated fast depolarization-mediated signals induced by thalamic stimulation to 79.9 ± 6.5% of control (n = 4; *P < 0.05). In HCN2$^{-/-}$ littermates, xenon did not affect the fast depolarization-mediated signals (93.8 ± 7.5% of control; n = 5; ns = not significant).

both HCN and TASK channel-mediated currents is the most efficient way to modulate the membrane potential,[56] the absence of a xenon-induced effect on TASK channels may explain our findings that neither resting membrane potential nor threshold or frequency of action potentials was changed using relevant concentrations of xenon. However, our data show that xenon decreases the inward current that would normally be active at hyperpolarized potentials (I_h) and consequently may stabilize thalamocortical neurons in the "down" state.

The I_h current mediated by HCN-channels is essential to control excitability, electrical responsiveness of cells, and

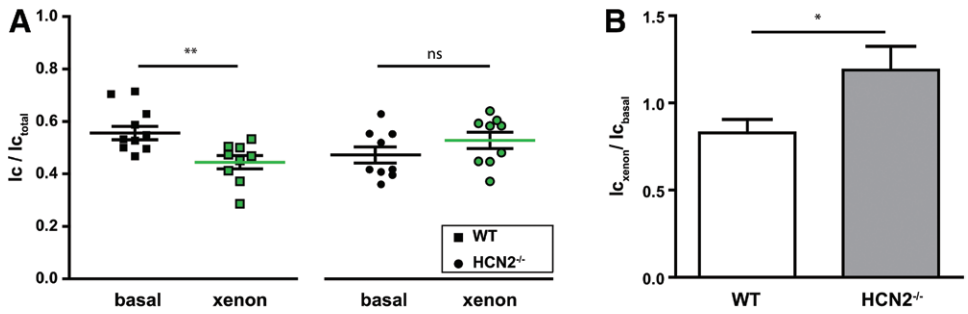

Fig. 7. Modified open-field test to evaluate the xenon-mediated effect on hyperpolarization-activated, cyclic nucleotide-gated cation channels type 2 (HCN2) channels *in vivo*. (*A*) The ratio of lines crossed (lc)/total lines crossed (lc_{total}) of each experiment was plotted for HCN wild-type (WT; *squares*) and HCN2$^{-/-}$ littermates (*circles*) under basal conditions (*black*; WT, 0.6 ± 0.0; HCN2$^{-/-}$, 0.5 ± 0.0) and xenon treatment (*green;* WT, 0.4 ± 0.0; HCN2$^{-/-}$, 0.5 ± 0.0) for every animal. The *lines* indicate mean and SEM. A significant reduction of lines crossed could be observed for WT mice under xenon treatment but nor for HCN2$^{-/-}$ littermates. $^{**}P < 0.01$. (*B*) The xenon effect was plotted as the ratio of lines crossed under xenon treatment (lc_{xenon}) compared with lines crossed under basal conditions (lc_{basal}) for WT (*white bar;* 0.8 ± 0.1) and HCN2$^{-/-}$ littermates (*gray bar;* 1.2 ± 0.1) as mean ± SEM. WT animals showed a reduced number of lines crossed compared with their HCN2$^{-/-}$ littermates. $^{*}P < 0.05$. ns = not significantly different.

oscillatory activity.[52,57,58] I_h currents activate partially at rest, thereby contributing to the resting membrane potential. In addition, they counteract both membrane hyperpolarization and depolarization by producing a depolarizing inward current or by facilitating hyperpolarization.[48] Xenon exerted two effects on native HCN channels in thalamocortical neurons: a hyperpolarizing shift in the voltage dependence of activation and a pronounced inhibition of the maximal I_h current amplitude. As a result, the use of xenon increases the chance of HCN channel closing in thalamocortical neurons under resting conditions. A blockade of I_h currents in thalamocortical neurons is described for intravenous[12] and volatile anesthetics.[13,52] This action may represent an important mechanism of anesthetic-induced unconsciousness as HCN channels are closely involved in the generation of synchronized neuronal oscillations in thalamocortical network, occurring during sleep.[59]

Thalamocortical neurons show a depolarizing sag, a low-threshold burst of action potentials and an after-burst depolarization in response to hyperpolarizing current injection.[60] Xenon decreased the depolarizing sag amplitude and increased the delay of rebound excitation. At the same time, HCN2-dependent I_h conductance[8] mediated the depolarizing sag and its amplitude correlated with the delay time of rebound spike firing in thalamocortical neurons.[12] These posthyperpolarization rebound bursts excite cortical pyramidal neurons.[59] Hence, impaired rebound bursting may lead to reduced cortical excitation and, thus, result in attenuated cortical depolarization, after thalamic stimulation.

Among the different HCN channel isoforms, HCN2 and HCN4 are most common in thalamocortical neurons,[32,49] whereas gene deletion studies indicate that HCN2 is the predominant isoform.[8] The fast activation time constant we observed for I_h currents in thalamocortical cells is consistent with fast activation time constants for HCN2, but not for HCN4-mediated currents in heterologous expression systems.[30,48,61] We found that xenon exerted similar effects on mHCN2-generated I_h currents compared with I_h currents recorded from thalamocortical neurons, suggesting that the effects observed for native currents resulted from modulation of HCN2 channels.

A characteristic of native and recombinant HCN channels is their modulation by cAMP.[48,58] In our study, a saturating concentration of cAMP produced a right-shift in $V_{1/2}$ of ≈12 mV for I_h currents generated by native HCN channels and a right-shift of ≈16 mV for currents conducted by heterologously expressed mHCN2 channels. Although the assembly of isoforms affects the sensitivity to cAMP, our results are consistent with various studies describing a cAMP-mediated depolarization shift of 7[62] to 28 mV[63] in native HCN channels and 2 to 5 mV[30] in recombinant HCN channels. In addition, cAMP accelerates activation kinetics[58] and enhances I_h currents. Interestingly, under conditions where the cytoplasm was saturated with cAMP, xenon failed to impair HCN channel function in both native HCN and recombinant HCN2 channels. This finding suggests that xenon may exert its actions on HCN channels through the modulation of intracellular cAMP. Although not significant, we observed a small decrease in the basal cAMP level after xenon administration. This trend toward a decrease in cAMP levels suggests that xenon inhibits adenylyl cyclase or increases phosphodiesterase activity. Volatile anesthetics inhibit adenylyl cyclase in adipocytes[64] and neuroblastoma cells.[65] A more recent study shows an isoflurane-dependent effect on adenylyl cyclase activity in *Caenorhabditis elegans*.[66] Furthermore, previous observations describe effects of xenon on enzymes such as the calcium ATPase[67] and protein kinase C.[68] Our data, however, do not allow for a definitive conclusion, and further research is required.

VSDI revealed a xenon-induced impairment of thalamocortical signal propagation. To determine whether the observed antagonism of HCN2 channels contributed to the reduced thalamocortical signal propagation, we performed VSDI experiments in HCN2$^{-/-}$ mice. Thalamocortical neurons

from HCN2$^{-/-}$ mice show a profound loss of I_h,[8] indicative of HCN2 channels mediating I_h currents in these neurons. In slices derived from HCN2$^{-/-}$ mice, xenon did not impair stimulation-evoked thalamocortical signal propagation. This strongly supports our hypothesis that xenon impairs thalamocortical connectivity by attenuating HCN2 channel functionality. Whether HCN channels enhance or inhibit synaptic transmission is debatable.[69–73] In the hippocampus, however, cyclic monophosphate–induced HCN channel activation seemed to increase presynaptic glutamate release.[71] Thus, the observed xenon-induced cAMP-dependent impairment of HCN channel function could account for decreased glutamate release from thalamocortical neurons at cortical synapses. This mechanism might explain the HCN channel–dependent impairment of thalamocortical connectivity by xenon. There is general agreement that a molecular target is important to the anesthetic state if it is modulated by anesthetics at clinically relevant concentrations, expressed at distinct anatomical locations, and resistant to the anesthetic's hypnotic/sedating effects that can be found in the absence of the molecular target. Cortical HCN1 channels fulfilled all three prerequisites using ketamine as anesthetic.[74,75] In line with these observations, our results clearly demonstrated *in vitro* and *in vivo* that HCN2 channels in the thalamus are an important molecular target for xenon-induced anesthesia. In mice lacking HCN2 channels and, therefore, under conditions where xenon failed to inhibit thalamocortical signal propagation, we could not find a sedating effect of xenon. However, at least under experimental conditions, modulation of thalamocortical connectivity seemed to be crucial for the xenon-induced anesthetic state.

In summary, we demonstrated that xenon depresses thalamocortical signal propagation. We provided evidence that this effect is, at least partially, mediated by a cAMP-dependent antagonism of xenon against HCN2 channels. Because xenon had no sedating effects on HCN2$^{-/-}$ mice and a depression of thalamocortical signal propagation seems to underlie the mechanisms of loss of consciousness, we conclude that an antagonism against HCN2 in the ventrobasal thalamus could contribute to the anesthetic action of xenon.

Acknowledgments

This work has been supported by grant no. HA5331/2-2 and the Sonderforschungsbereich 870 (SFB 870) from the German Research Society ("Deutsche Forschungsgemeinschaft", Bonn, Germany) and by a grant from the faculty of medicine of the Technical University Munich (Kommission klinische Forschung der TU Muenchen, Munich, Germany; KKF-B-3/12).

Competing Interests

The authors declare no competing interests.

Correspondence

Address correspondence to Dr. Kratzer: Department of Anesthesiology, Klinikum rechts der Isar, Technische Universität München, Ismaninger Straße 22, 81675 Munich, Germany. s.kratzer@lrz.tu-muenchen.de. Information on purchasing reprints may be found at www.anesthesiology.org or on the masthead page at the beginning of this issue. Anesthesiology's articles are made freely accessible to all readers, for personal use only, 6 months from the cover date of the issue.

References

1. Alkire MT: Probing the mind: anesthesia and neuroimaging. Clin Pharmacol Ther 2008; 84:149–52
2. Alkire MT, Miller J: General anesthesia and the neural correlates of consciousness. Prog Brain Res 2005; 150:229–44
3. Sherman SM: Thalamic relays and cortical functioning. Prog Brain Res 2005; 149:107–26
4. McCormick DA, Bal T: Sleep and arousal: Thalamocortical mechanisms. Annu Rev Neurosci 1997; 20:185–215
5. Steriade M, Jones EG, McCormick DA: Thalamus. Amsterdam, Elsevier, 1997
6. Sherman SM, Guillery RW: Functional organization of thalamocortical relays. J Neurophysiol 1996; 76:1367–95
7. Postea O, Biel M: Exploring HCN channels as novel drug targets. Nat Rev Drug Discov 2011; 10:903–14
8. Ludwig A, Budde T, Stieber J, Moosmang S, Wahl C, Holthoff K, Langebartels A, Wotjak C, Munsch T, Zong X, Feil S, Feil R, Lancel M, Chien KR, Konnerth A, Pape HC, Biel M, Hofmann F: Absence epilepsy and sinus dysrhythmia in mice lacking the pacemaker channel HCN2. EMBO J 2003; 22:216–24
9. Biel M, Wahl-Schott C, Michalakis S, Zong X: Hyperpolarization-activated cation channels: From genes to function. Physiol Rev 2009; 89:847–85
10. Derwall M, Coburn M, Rex S, Hein M, Rossaint R, Fries M: Xenon: Recent developments and future perspectives. Minerva Anestesiol 2009; 75:37–45
11. Rex S, Schaefer W, Meyer PH, Rossaint R, Boy C, Setani K, Büll U, Baumert JH: Positron emission tomography study of regional cerebral metabolism during general anesthesia with xenon in humans. Anesthesiology 2006; 105:936–43
12. Ying SW, Abbas SY, Harrison NL, Goldstein PA: Propofol block of I(h) contributes to the suppression of neuronal excitability and rhythmic burst firing in thalamocortical neurons. Eur J Neurosci 2006; 23:465–80
13. Ries CR, Puil E: Ionic mechanism of isoflurane's actions on thalamocortical neurons. J Neurophysiol 1999; 81:1802–9
14. Eckle VS, Digruccio MR, Uebele VN, Renger JJ, Todorovic SM: Inhibition of T-type calcium current in rat thalamocortical neurons by isoflurane. Neuropharmacology 2012; 63:266–73
15. Franks NP, Dickinson R, de Sousa SL, Hall AC, Lieb WR: How does xenon produce anaesthesia? Nature 1998; 396:324
16. Plested AJ, Wildman SS, Lieb WR, Franks NP: Determinants of the sensitivity of AMPA receptors to xenon. Anesthesiology 2004; 100:347–58
17. de Sousa SL, Dickinson R, Lieb WR, Franks NP: Contrasting synaptic actions of the inhalational general anesthetics isoflurane and xenon. Anesthesiology 2000; 92:1055–66
18. Haseneder R, Kratzer S, Kochs E, Eckle VS, Zieglgänsberger W, Rammes G: Xenon reduces N-methyl-D-aspartate and alpha-amino-3-hydroxy-5-methyl-4-isoxazolepropionic acid receptor-mediated synaptic transmission in the amygdala. Anesthesiology 2008; 109:998–1006
19. Haseneder R, Kratzer S, Kochs E, Mattusch C, Eder M, Rammes G: Xenon attenuates excitatory synaptic transmission in the rodent prefrontal cortex and spinal cord dorsal horn. Anesthesiology 2009; 111:1297–307
20. Agmon A, Connors BW: Thalamocortical responses of mouse somatosensory (barrel) cortex *in vitro*. Neuroscience 1991; 41:365–79
21. Aghajanian GK, Rasmussen K: Intracellular studies in the facial nucleus illustrating a simple new method for obtaining viable motoneurons in adult rat brain slices. Synapse 1989; 3:331–8

22. Stepan J, Dine J, Fenzl T, Polta SA, von Wolff G, Wotjak CT, Eder M: Entorhinal theta-frequency input to the dentate gyrus trisynaptically evokes hippocampal CA1 LTP. Front Neural Circuits 2012; 6:64
23. Dodt HU, Zieglgänsberger W: Visualizing unstained neurons in living brain slices by infrared DIC-videomicroscopy. Brain Res 1990; 537:333–6
24. Frick A, Zieglgänsberger W, Dodt HU: Glutamate receptors form hot spots on apical dendrites of neocortical pyramidal neurons. J Neurophysiol 2001; 86:1412–21
25. Zong X, Eckert C, Yuan H, Wahl-Schott C, Abicht H, Fang L, Li R, Mistrik P, Gerstner A, Much B, Baumann L, Michalakis S, Zeng R, Chen Z, Biel M: A novel mechanism of modulation of hyperpolarization-activated cyclic nucleotide-gated channels by Src kinase. J Biol Chem 2005; 280:34224–32
26. Cheng VY, Martin LJ, Elliott EM, Kim JH, Mount HT, Taverna FA, Roder JC, Macdonald JF, Bhambri A, Collinson N, Wafford KA, Orser BA: Alpha5GABAA receptors mediate the amnestic but not sedative-hypnotic effects of the general anesthetic etomidate. J Neurosci 2006; 26:3713–20
27. Hill MR, Greenfield SA: Characterization of early cortical population response to thalamocortical input *in vitro*. Front Neurosci 2013; 7:273
28. Chaplan SR, Guo HQ, Lee DH, Luo L, Liu C, Kuei C, Velumian AA, Butler MP, Brown SM, Dubin AE: Neuronal hyperpolarization-activated pacemaker channels drive neuropathic pain. J Neurosci 2003; 23:1169–78
29. Ishii TM, Takano M, Xie LH, Noma A, Ohmori H: Molecular characterization of the hyperpolarization-activated cation channel in rabbit heart sinoatrial node. J Biol Chem 1999; 274:12835–9
30. Ludwig A, Zong X, Stieber J, Hullin R, Hofmann F, Biel M: Two pacemaker channels from human heart with profoundly different activation kinetics. EMBO J 1999; 18:2323–9
31. DiFrancesco D, Tortora P: Direct activation of cardiac pacemaker channels by intracellular cyclic AMP. Nature 1991; 351:145–7
32. Notomi T, Shigemoto R: Immunohistochemical localization of Ih channel subunits, HCN1-4, in the rat brain. J Comp Neurol 2004; 471:241–76
33. Cullen SC, Eger EI II, Cullen BF, Gregory P: Observations on the anesthetic effect of the combination of xenon and halothane. Anesthesiology 1969; 31:305–9
34. Nakata Y, Goto T, Ishiguro Y, Terui K, Kawakami H, Santo M, Niimi Y, Morita S: Minimum alveolar concentration (MAC) of xenon with sevoflurane in humans. Anesthesiology 2001; 94:611–4
35. Weathersby PK, Homer LD: Solubility of inert gases in biological fluids and tissues: a review. Undersea Biomed Res 1980; 7:277–96
36. Koblin DD, Fang Z, Eger EI II, Laster MJ, Gong D, Ionescu P, Halsey MJ, Trudell JR: Minimum alveolar concentrations of noble gases, nitrogen, and sulfur hexafluoride in rats: helium and neon as nonimmobilizers (nonanesthetics). Anesth Analg 1998; 87:419–24
37. Yuste R, Tank DW, Kleinfeld D: Functional study of the rat cortical microcircuitry with voltage-sensitive dye imaging of neocortical slices. Cereb Cortex 1997; 7:546–58
38. Guillery RW: Anatomical evidence concerning the role of the thalamus in corticocortical communication: A brief review. J Anat 1995; 187 (Pt 3):583–92
39. Andersen P, Eccles JC, Sears TA: The ventro-basal complex of the thalamus: Types of cells, their responses and their functional organization. J Physiol 1964; 174:370–99
40. Lee CC, Sherman SM: Synaptic properties of thalamic and intracortical inputs to layer 4 of the first- and higher-order cortical areas in the auditory and somatosensory systems. J Neurophysiol 2008; 100:317–26
41. Kanyshkova T, Pawlowski M, Meuth P, Dubé C, Bender RA, Brewster AL, Baumann A, Baram TZ, Pape HC, Budde T: Postnatal expression pattern of HCN channel isoforms in thalamic neurons: Relationship to maturation of thalamocortical oscillations. J Neurosci 2009; 29:8847–57
42. Notomi T, Shigemoto R: Immunohistochemical localization of Ih channel subunits, HCN1-4, in the rat brain. J Comp Neurol 2004; 471:241–76
43. Haseneder R, Kratzer S, Kochs E, Höfelmann D, Auberson Y, Eder M, Rammes G: The xenon-mediated antagonism against the NMDA receptor is non-selective for receptors containing either NR2A or NR2B subunits in the mouse amygdala. Eur J Pharmacol 2009; 619:33–7
44. Franks NP: General anaesthesia: from molecular targets to neuronal pathways of sleep and arousal. Nat Rev Neurosci 2008; 9:370–86
45. Lüthi A, McCormick DA: Ca(2+)-mediated up-regulation of Ih in the thalamus. How cell-intrinsic ionic currents may shape network activity. Ann N Y Acad Sci 1999; 868:765–9
46. Steriade M, McCormick DA, Sejnowski TJ: Thalamocortical oscillations in the sleeping and aroused brain. Science 1993; 262:679–85
47. Huguenard JR, McCormick DA: Thalamic synchrony and dynamic regulation of global forebrain oscillations. Trends Neurosci 2007; 30:350–6
48. Biel M, Wahl-Schott C, Michalakis S, Zong X: Hyperpolarization-activated cation channels: From genes to function. Physiol Rev 2009; 89:847–85
49. Moosmang S, Biel M, Hofmann F, Ludwig A: Differential distribution of four hyperpolarization-activated cation channels in mouse brain. Biol Chem 1999; 380:975–80
50. Kim J, Wei DS, Hoffman DA: Kv4 potassium channel subunits control action potential repolarization and frequency-dependent broadening in rat hippocampal CA1 pyramidal neurones. J Physiol 2005; 569(Pt 1):41–57
51. Goldstein SA, Bockenhauer D, O'Kelly I, Zilberberg N: Potassium leak channels and the KCNK family of two-P-domain subunits. Nat Rev Neurosci 2001; 2:175–84
52. Budde T, Coulon P, Pawlowski M, Meuth P, Kanyshkova T, Japes A, Meuth SG, Pape HC: Reciprocal modulation of I (h) and I (TASK) in thalamocortical relay neurons by halothane. Pflugers Arch 2008; 456:1061–73
53. Patel AJ, Honoré E, Lesage F, Fink M, Romey G, Lazdunski M: Inhalational anesthetics activate two-pore-domain background K+ channels. Nat Neurosci 1999; 2:422–6
54. Patel AJ, Honoré E: Anesthetic-sensitive 2P domain K+ channels. Anesthesiology 2001; 95:1013–21
55. Franks NP, Honoré E: The TREK K2P channels and their role in general anaesthesia and neuroprotection. Trends Pharmacol Sci 2004; 25:601–8
56. Meuth SG, Aller MI, Munsch T, Schuhmacher T, Seidenbecher T, Meuth P, Kleinschnitz C, Pape HC, Wiendl H, Wisden W, Budde T: The contribution of TWIK-related acid-sensitive K+-containing channels to the function of dorsal lateral geniculate thalamocortical relay neurons. Mol Pharmacol 2006; 69:1468–76
57. Pape HC, McCormick DA: Ionic mechanisms of modulatory brain stem influences in the thalamus. J Basic Clin Physiol Pharmacol 1990; 1:107–17
58. Pape HC: Queer current and pacemaker: The hyperpolarization-activated cation current in neurons. Annu Rev Physiol 1996; 58:299–327
59. Wahl-Schott C, Biel M: HCN channels: structure, cellular regulation and physiological function. Cell Mol Life Sci 2009; 66:470–94
60. Ying SW, Goldstein PA: Propofol suppresses synaptic responsiveness of somatosensory relay neurons to excitatory input by potentiating GABA(A) receptor chloride channels. Mol Pain 2005; 1:2
61. Seifert R, Scholten A, Gauss R, Mincheva A, Lichter P, Kaupp UB: Molecular characterization of a slowly gating

human hyperpolarization-activated channel predominantly expressed in thalamus, heart, and testis. Proc Natl Acad Sci U S A 1999; 96:9391–6

62. Pape HC, McCormick DA: Noradrenaline and serotonin selectively modulate thalamic burst firing by enhancing a hyperpolarization-activated cation current. Nature 1989; 340:715–8
63. Vargas G, Lucero MT: Dopamine modulates inwardly rectifying hyperpolarization-activated current (Ih) in cultured rat olfactory receptor neurons. J Neurophysiol 1999; 81:149–58
64. Ohlson KB, Shabalina IG, Lennström K, Backlund EC, Mohell N, Bronnikov GE, Lindahl SG, Cannon B, Nedergaard J: Inhibitory effects of halothane on the thermogenic pathway in brown adipocytes: Localization to adenylyl cyclase and mitochondrial fatty acid oxidation. Biochem Pharmacol 2004; 68:463–77
65. Kuroda M, Yoshikawa D, Nishikawa K, Saito S, Goto F: Volatile anesthetics inhibit calcitonin gene-related peptide receptor-mediated responses in pithed rats and human neuroblastoma cells. J Pharmacol Exp Ther 2004; 311:1016–22
66. Saifee O, Metz LB, Nonet ML, Crowder CM: A gain-of-function mutation in adenylate cyclase confers isoflurane resistance in Caenorhabditis elegans. Anesthesiology 2011; 115:1162–71
67. Franks JJ, Horn JL, Janicki PK, Singh G: Halothane, isoflurane, xenon, and nitrous oxide inhibit calcium ATPase pump activity in rat brain synaptic plasma membranes. Anesthesiology 1995; 82:108–17
68. Weber NC, Toma O, Wolter JI, Obal D, Müllenheim J, Preckel B, Schlack W: The noble gas xenon induces pharmacological preconditioning in the rat heart *in vivo via* induction of PKC-epsilon and p38 MAPK. Br J Pharmacol 2005; 144:123–32
69. Beaumont V, Zucker RS: Enhancement of synaptic transmission by cyclic AMP modulation of presynaptic Ih channels. Nat Neurosci 2000; 3:133–41
70. Beaumont V, Zhong N, Froemke RC, Ball RW, Zucker RS: Temporal synaptic tagging by I(h) activation and actin: involvement in long-term facilitation and cAMP-induced synaptic enhancement. Neuron 2002; 33:601–13
71. Neitz A, Mergia E, Eysel UT, Koesling D, Mittmann T: Presynaptic nitric oxide/cGMP facilitates glutamate release *via* hyperpolarization-activated cyclic nucleotide-gated channels in the hippocampus. Eur J Neurosci 2011; 33:1611–21
72. Boyes J, Bolam JP, Shigemoto R, Stanford IM: Functional presynaptic HCN channels in the rat globus pallidus. Eur J Neurosci 2007; 25:2081–92
73. Huang Z, Lujan R, Kadurin I, Uebele VN, Renger JJ, Dolphin AC, Shah MM: Presynaptic HCN1 channels regulate Cav3.2 activity and neurotransmission at select cortical synapses. Nat Neurosci 2011; 14:478–86
74. Zhou C, Douglas JE, Kumar NN, Shu S, Bayliss DA, Chen X: Forebrain HCN1 channels contribute to hypnotic actions of ketamine. Anesthesiology 2013; 118:785–95
75. Chen X, Shu S, Bayliss DA: HCN1 channel subunits are a molecular substrate for hypnotic actions of ketamine. J Neurosci 2009; 29:600–9